Imaging Science in Dentistry 2024; 54: 191-9
https://doi.org/10.5624/isd.20240016

Impact of the spatial orientation of the patient's head, metal artifact reduction, and tube current on cone-beam computed tomography artifact expression adjacent to a dental implant: A laboratory study using a simulated surgical guide

Matheus Barros-Costa[1], Julia Ramos Barros-Candido[1], Matheus Sampaio-Oliveira[1], Deborah Queiroz Freitas[1], Alexander Tadeu Sverzut[2], Matheus L Oliveira[1,*]

[1]*Division of Oral Radiology, Department of Oral Diagnosis, Piracicaba Dental School, University of Campinas, Piracicaba, SP, Brazil*
[2]*Division of Oral and Maxillofacial Surgery, Department of Oral Diagnosis, Piracicaba Dental School, University of Campinas, Piracicaba, SP, Brazil*

ABSTRACT

Purpose: The aim of this study was to evaluate image artifacts in the vicinity of dental implants in cone-beam computed tomography (CBCT) scans obtained with different spatial orientations, tube current levels, and metal artifact reduction algorithm (MAR) conditions.

Materials and Methods: One dental implant and 2 tubes filled with a radiopaque solution were placed in the posterior region of a mandible using a surgical guide to ensure parallel alignment. CBCT scans were acquired with the mandible in 2 spatial orientations in relation to the X-ray projection plane (standard and modified) at 3 tube current levels: 5, 8, and 11 mA. CBCT scans were repeated without the implant and were reconstructed with and without MAR. The mean voxel and noise values of each tube were obtained and compared using multi-way analysis of variance and the Tukey test ($\alpha = 0.05$).

Results: Mean voxel values were significantly higher and noise values were significantly lower in the modified orientation than in the standard orientation ($P < 0.05$). MAR activation and tube current levels did not show significant differences in most cases of the modified spatial orientation and in the absence of the dental implant ($P > 0.05$).

Conclusion: Modifying the spatial orientation of the head increased brightness and reduced spatial orientation noise in adjacent regions of a dental implant, with no influence from the tube current level and MAR. ***(Imaging Sci Dent 2024; 54: 191-9)***

KEY WORDS: Cone-Beam Computed Tomography; Artifacts; Patient Positioning; Dental Implants; Titanium

Introduction

Cone-beam computed tomography (CBCT) offers a 3-dimensional evaluation of the oral and maxillofacial structures. This imaging technique is commonly utilized in dentistry when traditional radiographs are inadequate for certain diagnostic tasks due to structural overlap. When the principles of justification and optimization are respected, CBCT can be considered as an aid in dental diagnosis.[1-4] However, despite its numerous benefits, a significant inherent drawback of CBCT is the occurrence of image artifacts.

The presence of high-density materials inside and/or outside the scanned region in CBCT has been identified as a significant source of artifacts. These artifacts can appear as hypodense and hyperdense bands and streaks, resulting from X-ray beam hardening and photon starvation. Dental implants, restorative materials, and endodontic components, commonly found in the oral cavity, are frequent

This study was supported by the Grants #2022/02143-2 and #2018/18663-0, São Paulo Research Foundation (FAPESP).
Received January 30, 2024; Revised March 26, 2024; Accepted April 5, 2024
Published online May 7, 2024
*Correspondence to : Prof. Matheus L Oliveira
Division of Oral Radiology, Department of Oral Diagnosis, Piracicaba Dental School, University of Campinas, Av. Limeira, 901, Zip Code 13414-903, Piracicaba, São Paulo, Brazil
Tel) 55-19-2106-5267, E-mail) matheuso@unicamp.br

Imaging Science in Dentistry · pISSN 2233-7822 eISSN 2233-7830

culprits behind these image artifacts. The deterioration in image quality can affect areas surrounding the source object, potentially compromising diagnostic accuracy.[5-8] Numerous strategies to reduce image artifacts have been explored, including modifications to acquisition protocols and the implementation of artifact reduction algorithms.[5,6,9-12] The tube current, also referred to as milliamperage (mA) level, is directly and linearly related to the number of X-ray photons and therefore affects the noise level in CBCT scans.

The degradation of image quality caused by artifacts is observed in the path of X-rays that pass through an object, which is the opposite of what occurs in back-projection reconstruction. This technique is a mathematical method used to reconstruct 3-dimensional (3D) images from various 2-dimensional (2D) X-ray projections taken around the object being scanned. These projections are compromised by the presence of high-density materials, which introduce errors in the reconstruction of 3D images due to diminished signal reception by the receptor.[13] Additionally, most CBCT machines are designed in a way that results in a predominantly axial distribution of artifacts. Consequently, it is crucial to assess how the spatial orientation of a patient's head might influence the quantitative representation of image artifacts near dental implants in CBCT. Therefore, the purpose of this study was to evaluate the potential impact of the patient's head orientation, the use of metal artifact reduction techniques, and the level of tube current on the manifestation of image artifacts near a dental implant in CBCT examinations.

Materials and Methods

This study was carried out as an experimental and prospective investigation and received approval from the local Institutional Research Review Board (protocol #56244 722.5.0000.5418).

Phantom preparation

A dry human skull was covered with a layer of MixD[14] to simulate a patient's soft tissues. MixD was custom-made by blending fractional portions of 304 g of paraffin wax, 152 g of polyethylene, 32 g of magnesium oxide, and 12 g of titanium dioxide, based on previously published methodologies.[14,15]

A synthetic mandible composed of polyurethane and barium sulfate (Nacional Ossos, São Paulo, Brazil) was also used to construct the phantom. Two polypropylene tubes of 0.2 mL were filled with a custom-made aqueous solution of dipotassium hydrogen phosphate (K_2HPO_4) with a concentration of 1000 mg/mL. K_2HPO_4 is a salt that has demonstrated a satisfactory ability to simulate dental mineralized tissues.[16,17]

The 2 propylene tubes and a titanium dental implant with dimensions of 4 × 11 mm (Neodent, Curitiba, Brazil) were installed in the left posterior region of the mandible. To achieve perfect parallel alignment between the 2 tubes and the dental implant, a virtual planning process was conducted using BlueSkyPlan 4.9.4 software (BlueSky Bio, Libertyville, IL, USA) and a surgical guide was manufactured. One tube was positioned anterior to the dental implant, while the other was positioned posterior to it (Fig. 1). The mandible was then affixed to the skull to simulate the patient's head.

Image acquisition

Using an OP300 Maxio unit (Instrumentarium, Tuusula, Finland) operating at 90 kVp, with a voxel size of 0.125 mm, a field-of-view of 5 × 5 cm and 3 levels of tube current (5, 8, and 11 mA), 3 repeated CBCT scans were acquired with the phantom head positioned in 2 distinct spatial orientations relative to the X-ray projection plane: standard and modified. Triplicate scans were obtained to ensure the reproducibility of voxel values.

The standard spatial orientation was the same as that used for patients, with both tubes and the dental implant positioned upright, perpendicular to the axial plane (Fig. 2A). The modified spatial orientation was achieved by tilting the phantom head 90 degrees backward, aligning the tubes and dental implant parallel to the axial plane (Fig. 2B). Subsequently, the dental implant was removed from the mandible, and all CBCT scans were repeated. All CBCT scans were then reconstructed both with and without the activation of the metal artifact reduction (MAR) algorithm. The position of the phantom remained consistent in the CBCT unit for each spatial orientation and implant condition to eliminate potential bias from voxel value variability. Consequently, a total of 72 CBCT scans were obtained, calculated as follows: 3 repetitions × 2 spatial orientations of the head × 2 dental implant conditions (with and without) × 2 MAR activation states (with and without) × 3 levels of tube current (Fig. 3).

Image assessment

The CBCT scans were exported in DICOM file format, and those obtained with the phantom head in the modified spatial orientation were imported into OnDemand 3D software (Cybermed, Seoul, Korea). These scans were

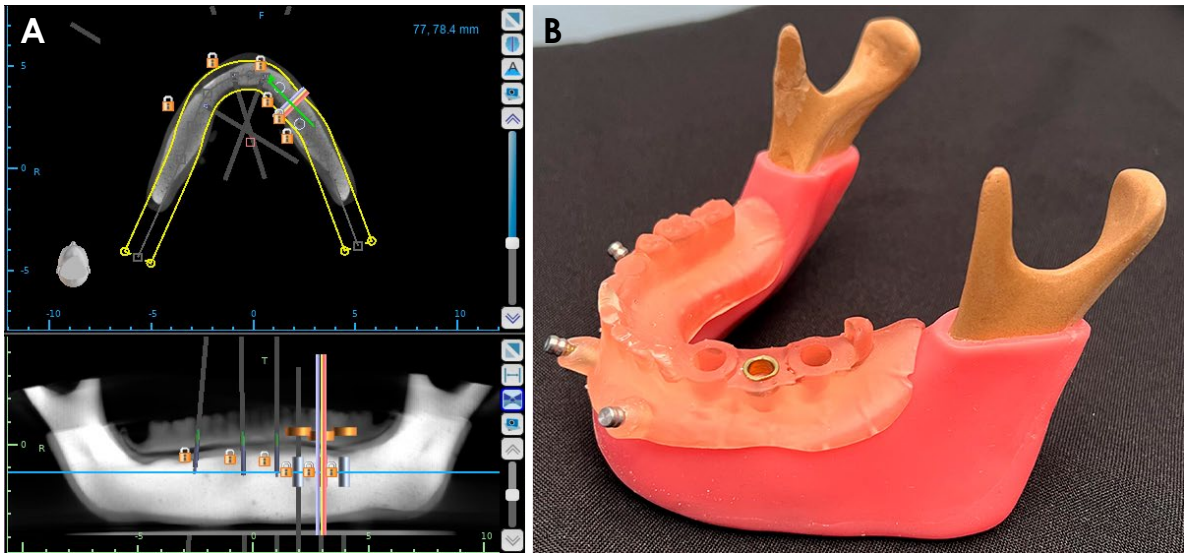

Fig. 1. Virtual planning model design. A. Cone-beam computed tomographic axial and panoramic reconstructions demonstrate perfect alignment between the two regions and the dental implant. B. Photograph of the surgical guide, which is precisely adapted to the synthetic mandible of the phantom.

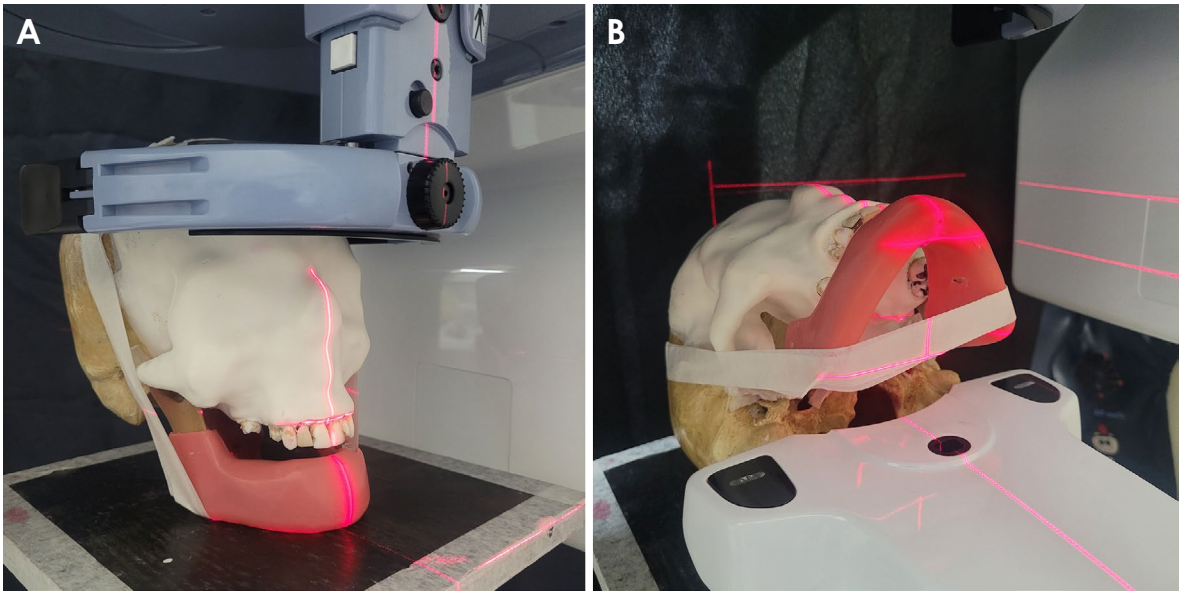

Fig. 2. Photographs of the phantom head positioned in the cone-beam computed tomography unit, showing two distinct spatial orientations relative to the X-ray projection plane: A. Standard orientation. B. Modified orientation.

then reoriented to align the longitudinal axis of 2 tubes and a dental implant to match those in the standard spatial orientation. From a practical standpoint, the axial anatomic plane of the phantom head was adjusted from the originally acquired coronal reconstructions to axial reconstructions. Following this, all CBCT scans were individually analyzed using ImageJ/Fiji software (National Institutes of Health, Bethesda, MD, USA). In the axial reconstruction at the most coronal level of the dental implant, a circular region of interest (ROI) measuring 3 mm^2 was selected at the center of each tube and extended through the next forty slices in the apical direction, creating a cylindrical ROI. The macro tool in ImageJ/Fiji was utilized to standardize the positioning of the ROIs. Mean voxel values and standard deviations were calculated to evaluate image density and noise under different study conditions.

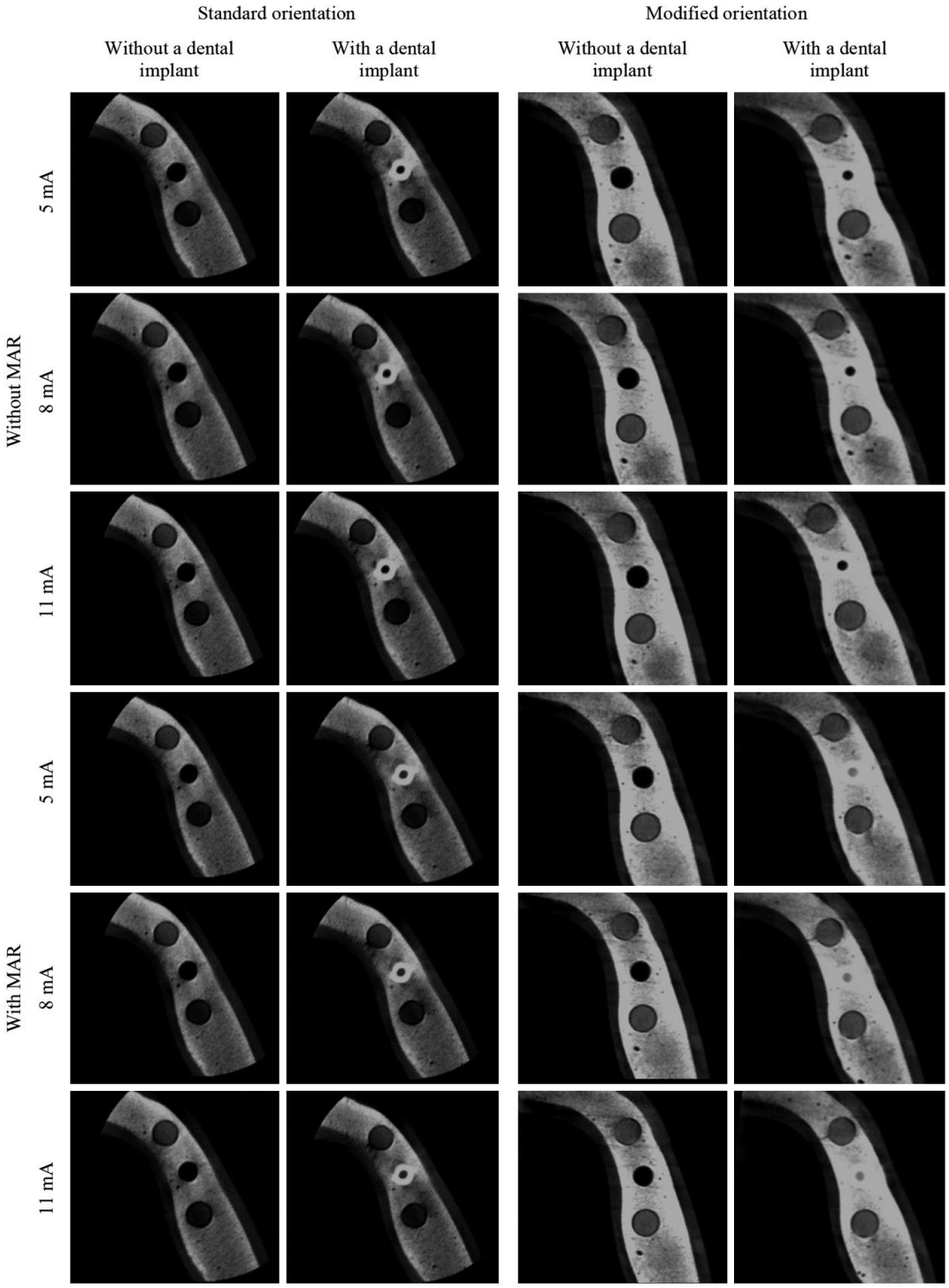

Fig. 3. Cone-beam computed tomographic axial reconstructions as a function of the spatial orientation of the head, dental implant condition, metal artifact reduction (MAR) activation, and tube current.

The mean voxel value indicates the average grayscale intensity of the voxels within the ROI, while the standard deviation measures the variability of these voxel values, which can be interpreted as noise in a homogeneous area. To assess reproducibility, 30% of the CBCT scans were randomly selected and independently evaluated by another examiner.

Statistical analysis

A power analysis was conducted to ensure adequate

Table 1. Voxel values of each region as a function of the spatial orientation of the head, dental implant condition, metal artifact reduction (MAR) activation, and tube current (mA)

	MAR	mA	Anterior region		Posterior region	
			Standard orientation	Modified orientation*	Standard orientation	Modified orientation*
Without dental implant	Without	5	1032 ± 4.62	1310 ± 5.32	430 ± 1.83	1409 ± 1.89[b]
		8	1027 ± 2.18	1306 ± 6.27	432 ± 2.56	1426 ± 3.18[a]
		11	1027 ± 1.98	1299 ± 1.25	431 ± 1.34	1427 ± 2.02[a]
	With	5	1032 ± 4.62	1316 ± 0.57	430 ± 1.83	1410 ± 1.15[b]
		8	1027 ± 2.18	1309 ± 5.83	432 ± 2.56	1425 ± 5.30[a]
		11	1027 ± 1.98	1303 ± 1.26[†]	431 ± 1.34	1427 ± 1.99[a]
With dental implant	Without	5	669 ± 2.72[†]	1188 ± 5.56[a†]	453 ± 1.96	1444 ± 5.43[c]
		8	667 ± 1.59[†]	1182 ± 2.44[a†]	457 ± 0.93	1457 ± 6.26[b]
		11	670 ± 1.88[†]	1171 ± 0.67[b†]	455 ± 1.83	1469 ± 3.64[a]
	With	5	849 ± 2.79[†‡]	1189 ± 5.40[a†]	450 ± 1.93	1445 ± 5.58[c]
		8	839 ± 3.49[†‡]	1182 ± 2.45[a†]	451 ± 1.30	1457 ± 6.27[b]
		11	840 ± 1.56[†‡]	1172 ± 0.66[b†]	452 ± 1.56	1469 ± 3.48[a]

*: $P<0.05$ compared to "standard orientation," [†]: $P<0.05$ compared to "without dental implant," [‡]: $P<0.05$ compared to "without MAR." Different letters indicate a significant difference between tube current levels within the same conditions of orientation, dental implant, and MAR ($P<0.05$).

statistical power for detecting significant effects or relationships between variables, with a significance level set at 5% ($\alpha=0.05$). This analysis took into account the minimum differences among the groups, the mean standard deviation, and the number of repetitions per group, resulting in a power of 90% (0.90). The intraclass correlation coefficient was utilized to assess the reproducibility of the examination. Multi-way analysis of variance with the *post hoc* Tukey test was employed to independently evaluate the image density and noise across different conditions for each region. These conditions included the spatial orientation of the head, the presence of a dental implant, MAR activation, and the level of tube current. All analyses were performed using SPSS software version 24.0 (IBM Corp, Armonk, NY, USA).

Results

The reproducibility, evaluated by the intraclass correlation coefficient, showed excellent agreement, with a mean of 0.98 (range, 0.97-0.99).

Table 1 displays the mean voxel values of the ROIs in the anterior and posterior regions of the dental implant under various study conditions. The mean voxel values were significantly higher in both regions when using the modified spatial orientation compared to the standard spatial orientation, given the same dental implant condition, MAR activation, and tube current level ($P<0.05$). The inclusion of a titanium dental implant resulted in significantly lower mean voxel values in the anterior region, regardless of the spatial orientation, MAR activation, and tube current level ($P<0.05$). Typically, MAR activation was associated with significantly higher mean voxel values in the anterior region when the phantom head was positioned in the standard spatial orientation and equipped with a dental implant, regardless of the tube current level ($P<0.05$). Generally, using 11 mA in the modified spatial orientation resulted in significantly lower and higher mean voxel values in the anterior and posterior regions, respectively.

Table 2 presents the noise values in the anterior and posterior regions under various conditions. Noise values were generally lower in the modified spatial orientation compared to the standard spatial orientation for both regions, with significant differences noted in most cases ($P<0.05$). The introduction of a dental implant resulted in significantly higher noise values in the standard spatial orientation ($P<0.05$). However, in the modified spatial orientation, only a few cases exhibited significantly higher values ($P<0.05$). The activation of MAR significantly reduced noise values in both regions, but only in the standard spatial orientation and when a dental implant was present, regardless of the tube current level ($P<0.05$). The tube current level significantly affected noise values in most scenarios involving the modified spatial orientation for both regions. Typically, 11 mA resulted in significantly higher noise val-

Table 2. Noise values of each region as a function of the spatial orientation of the head, dental implant condition, metal artifact reduction (MAR) activation, and tube current (mA)

	MAR	mA	Anterior region		Posterior region	
			Standard orientation	Modified orientation	Standard orientation	Modified orientation
Without dental implant	Without	5	154 ± 1.45	121 ± 8.97*	116 ± 2.42[a]	87 ± 6.03[a*]
		8	149 ± 3.99	115 ± 1.86*	106 ± 1.57[b]	84 ± 5.70[ab*]
		11	146 ± 1.17	114 ± 4.37*	103 ± 0.16[b]	78 ± 0.34[b*]
	With	5	154 ± 1.45	120 ± 9.28*	116 ± 2.42[a]	87 ± 5.69[a*]
		8	149 ± 3.99	114 ± 2.14*	106 ± 1.57[b]	79 ± 4.02[b*]
		11	146 ± 1.17	116 ± 4.20*	103 ± 0.16[b]	78 ± 0.44[b*]
With dental implant	Without	5	188 ± 1.19†	115 ± 1.45[b*]	130 ± 1.79†	96 ± 2.11[b*]
		8	180 ± 4.04†	129 ± 14.96[b*]	123 ± 1.51†	104 ± 9.26[b*†]
		11	180 ± 0.34†	152 ± 7.20[a*†]	121 ± 1.57†	126 ± 6.96[a†]
	With	5	173 ± 1.25†‡	115 ± 0.94[b*]	106 ± 2.61†‡	96 ± 2.46[b]
		8	163 ± 2.23†‡	129 ± 14.96[b*]	100 ± 0.58†‡	104 ± 9.53[b†]
		11	162 ± 0.75†‡	152 ± 7.10[a†]	96 ± 1.09†‡	126 ± 6.79[a*†]

*: $P<0.05$ compared to "standard orientation," †: $P<0.05$ compared to "without dental implant," ‡: $P<0.05$ compared to "without MAR." Different letters indicate a significant difference between tube current levels within the same conditions of orientation, dental implant, and MAR ($P<0.05$)

ues when a dental implant was present and significantly lower noise values when absent ($P<0.05$). In the standard spatial orientation, the tube current level significantly impacted noise values only in the posterior region and only when the dental implant was absent; in these instances, 5 mA led to significantly higher noise values ($P<0.05$).

Discussion

The impact of image artifacts on hindering or even invalidating diagnoses in dentistry is well-documented in the scientific literature.[5-10] Hypodense and hyperdense streaks can extend into the surrounding areas of high-density objects within the scanned region. The high attenuation and dispersion of X-rays during CBCT scans can impair primary reconstruction, leading to decreased image quality.[13,18,19] Diagnostic tasks such as the identification of vertical root fractures,[6,8-10] tooth resorption,[5,7] and bone defects[20] are particularly affected by the presence of artifacts. A previous study[6] has shown that image artifacts arising from adjacent or distant dental implants can mimic fracture lines and negatively affect the diagnosis of vertical root fractures, potentially leading to unnecessary tooth extraction. Another similar study[9] found that applying MAR and adjusting the tube current were ineffective for this diagnostic task. Regarding dental root resorption, a prior study[7] concluded that artifacts produced by teeth restored with a metal post also hindered the diagnosis of internal root resorption in adjacent teeth. Similarly, another study reported impairment in the detection of external root resorption due to artifacts generated near dental implants. Furthermore, the assessment of bone defects surrounding dental implants may be compromised by the presence of artifacts generated by the implants themselves.[20] The region surrounding high-density objects is most strongly affected by image artifacts, which served as the primary motivation for conducting the present study.

An increase in mean voxel values in the absence of a dental implant with the modified spatial orientation may indicate the indirect presence of hyperdense artifacts. These artifacts likely originate from parts of the skull located in the exomass, which is the area outside the field of view, but still between the X-ray source and the image receptor.[16,17] The decrease in noise values in the anterior and posterior regions around the dental implant, when using the modified spatial orientation, is likely due to the way the X-rays are projected in relation to the high-density object. The distribution of artifacts in the transverse plane of the dental implant is minimized in the modified spatial orientation because the original acquisition was in coronal reconstructions, which results in fewer image artifacts nearby. To the best of the authors' knowledge, current CBCT machines do not typically allow patients to adjust their head positioning as suggested in this study. However,

this experimental study yielded promising results by minimizing artifacts, which suggests that manufacturers should consider enhancing the flexibility of patient positioning relative to the X-ray projection plane in future designs of CBCT units.

A previous study suggested a slight tilt of the mandible relative to the axial plane to assess its potential impact on the expression of image artifacts. Interestingly, this adjustment led to a reduction in the artifacts produced by dental implants in the surrounding simulated soft tissue.[21] Similarly, Wanderley et al.[22] also modified the spatial orientation of the head to avoid artifacts generated by intracanal materials in the diagnosis of root fractures. Nevertheless, the authors concluded that this modification did not improve the diagnosis of vertical root fractures. The authors believe that the expression of artifacts in objects very close to high-density materials, such as intracanal fillings, is not influenced by head position adjustments due to the potentially low occurrence of beam-hardening and blooming artifacts.[23] Conversely, in another study, Wanderley et al.[24] evaluated the effect of the combined evaluation of CBCT scans obtained in standard and modified spatial orientations. They concluded that this approach improved the diagnosis of vertical root fractures in teeth with intracanal material.

The CBCT acquisition parameters significantly influence the manifestation of image artifacts. These parameters include tube current, tube voltage, C-arm rotation degree, voxel and field-of-view sizes, and MAR activation.[13,25-27] In this study, the tube current and MAR activation were specifically adjusted to explore how these changes affect the CBCT images when the head is positioned in two different spatial orientations. It is crucial to note that the tube voltage and C-arm rotation degree were constant settings on the CBCT unit used in this research. It was observed that changes in the tube current level notably affected the image quality at the modified position in the presence of a dental implant. However, the variations in noise levels did not exhibit a consistent pattern. This inconsistency might be attributed to the presence of the skull in the exomass at the modified spatial orientation, which could increase scattered radiation.[16,17] The increased dispersion of X-rays, due to additional structures, might account for the variability in noise levels under the same conditions. Moreover, MAR activation effectively reduced noise only in the standard position when a dental implant was present. According to the authors' hypothesis, MAR did not influence the outcomes when the dental implant was absent or when the head was in the modified spatial orientation. This lack of impact could be explained by the minimal artifact generation in these scenarios, which did not require significant reduction.

In light of the significant findings of this study, the authors recommend further research to assess the impact of modifying head spatial orientation in various clinical scenarios. For instance, an area of investigation could explore whether changes in spatial orientation enhance the diagnosis of vertical root fractures in teeth adjacent to dental implants. Additionally, altering the head's spatial orientation affects the areas exposed to X-rays. Therefore, it is also necessary to investigate the effective dose of radiation under different spatial orientations of the head.

Being an *in vitro* study, this research has inherent limitations related to the simulation of internal soft tissues and potential micro-movements. However, it is crucial to recognize that the experimental protocol employed in this study would not be feasible in human subjects due to the repeated use of ionizing radiation. In this study design, it was possible to conduct multiple CBCT scans and standardize both the sample and its positioning during these scans, which was essential for the type of evaluation performed. Furthermore, when interpreting the results, it is important to account for potential variations in CBCT machine specifications and imaging parameters across different manufacturers, as these may affect the effectiveness of spatial orientation modifications in reducing artifacts.

The method proposed in this laboratory study involved tilting the patient's head back by 90 degrees to mitigate implant-related image artifacts. However, this approach may not be directly applicable in real clinical settings due to practical limitations and patient discomfort. Despite these challenges, our findings offer promising insights that are of significant value to manufacturers in the imaging technology field, contributing to an understanding of how image artifacts form and appear. By demonstrating the effectiveness of this method under controlled laboratory conditions, we lay the groundwork for further exploration and refinement.

In conclusion, modifying the spatial orientation of the patient's head typically enhances brightness and reduces noise in the regions adjacent to a dental implant. The application of metal artifact reduction and adjustments to the tube current level, when the patient's head is positioned in this modified orientation, appear to have no significant impact on the adjacent regions of a dental implant. Further research is required to implement this methodology in diagnostic tasks.

Conflicts of Interest: None

Acknowledgments

In memoriam, the authors extend their deepest gratitude to Prof. Dr. Alexander Tadeu Sverzut for his invaluable contributions to this research.

References

1. Special Committee to Revise the Joint AAE/AAOMR Position Statement on use of CBCT in Endodontics. AAE and AAOMR joint position statement: use of cone beam computed tomography in endodontics 2015 update. Oral Surg Oral Med Oral Pathol Oral Radiol 2015; 120: 508-12.
2. Patel S, Brown J, Semper M, Abella F, Mannocci F. European Society of Endodontology position statement: use of cone beam computed tomography in endodontics: European society of endodontology (ESE) developed by. Int Endod J 2019; 52: 1675-8.
3. Patel S, Brown J, Pimentel T, Kelly RD, Abella F, Durack C. Cone beam computed tomography in endodontics - a review of the literature. Int Endod J 2019; 52: 1138-52.
4. Oenning AC, Jacobs R, Salmon B. ALADAIP, beyond ALARA and towards personalized optimization for paediatric cone-beam CT. Int J Paediatr Dent 2021; 31: 676-8.
5. Freitas DQ, Nascimento EHL, Vasconcelos TV, Noujeim M. Diagnosis of external root resorption in teeth close and distant to zirconium implants: influence of acquisition parameters and artefacts produced during cone beam computed tomography. Int Endod J 2019; 52: 866-73.
6. Freitas DQ, Vasconcelos TV, Noujeim M. Diagnosis of vertical root fracture in teeth close and distant to implant: an in vitro study to assess the influence of artifacts produced in cone beam computed tomography. Clin Oral Investig 2019; 23: 1263-70.
7. Gaêta-Araujo H, Nascimento EH, Oliveira-Santos N, Pinheiro MC, Coelho-Silva F, Oliveira-Santos C. Influence of adjacent teeth restored with metal posts in the detection of simulated internal root resorption using CBCT. Int Endod J 2020; 53: 1299-306.
8. Marinho Vieira LE, Diniz de Lima E, Peixoto LR, Oliveira Pinto MG, Sousa Melo SL, Oliveira ML, et al. Assessment of the influence of different intracanal materials on the detection of root fracture in birooted teeth by cone-beam computed tomography. J Endod 2020; 46: 264-70.
9. Fontenele RC, Farias Gomes A, Nejaim Y, Freitas DQ. Do the tube current and metal artifact reduction influence the diagnosis of vertical root fracture in a tooth positioned in the vicinity of a zirconium implant? A CBCT study. Clin Oral Investig 2021; 25: 2229-35.
10. Gaêta-Araujo H, Silva de Souza GQ, Freitas DQ, de Oliveira-Santos C. Optimization of tube current in cone-beam computed tomography for the detection of vertical root fractures with different intracanal materials. J Endod 2017; 43: 1668-73.
11. Nascimento EH, Fontenele RC, Santaella GM, Freitas DQ. Difference in the artefacts production and the performance of the metal artefact reduction (MAR) tool between the buccal and lingual cortical plates adjacent to zirconium dental implant. Dentomaxillofac Radiol 2019; 48: 20190058.
12. Fontenele RC, Nascimento EH, Santaella GM, Freitas DQ. Does the metal artifact reduction algorithm activation mode influence the magnitude of artifacts in CBCT images? Imaging Sci Dent 2020; 50: 23-30.
13. Schulze R, Heil U, Groß D, Bruellmann DD, Dranischnikow E, Schwanecke U, et al. Artefacts in CBCT: a review. Dentomaxillofac Radiol 2011; 40: 265-73.
14. Jones DE, Raine HC. Correspondence. Br J Radiol 1949; 22: 549-50.
15. Brand JW, Kuba RK, Braunreiter TC. An improved head-and-neck phantom for radiation dosimetry. Oral Surg Oral Med Oral Pathol 1989; 67: 338-46.
16. Oliveira ML, Tosoni GM, Lindsey DH, Mendoza K, Tetradis S, Mallya SM. Influence of anatomical location on CT numbers in cone beam computed tomography. Oral Surg Oral Med Oral Pathol Oral Radiol 2013; 115: 558-64.
17. Candemil AP, Salmon B, Freitas DQ, Ambrosano GM, Haiter-Neto F, Oliveira ML. Metallic materials in the exomass impair cone beam CT voxel values. Dentomaxillofac Radiol 2018; 47: 20180011.
18. Pauwels R, Stamatakis H, Bosmans H, Bogaerts R, Jacobs R, Horner K, et al. Quantification of metal artifacts on cone beam computed tomography images. Clin Oral Implants Res 2013; 24 Suppl A100: 94-9.
19. Pauwels R, Araki K, Siewerdsen JH, Thongvigitmanee SS. Technical aspects of dental CBCT: state of the art. Dentomaxillofac Radiol 2015; 44: 20140224.
20. Kuusisto N, Abushahba F, Syrjänen S, Huumonen S, Vallittu P, Närhi T. Zirconia implants interfere with the evaluation of peri-implant bone defects in cone beam computed tomography (CBCT) images even with artifact reduction, a pilot study. Dentomaxillofac Radiol 2023; 52: 20230252.
21. Khurana S, Parasher P, Creanga AG, Geha H. Effect of mandible phantom inclination in the axial plane on image quality in the presence of implant using cone-beam computer tomography. Cureus 2023; 15: e36630.
22. Wanderley VA, Freitas DQ, Haiter-Neto F, Oliveira ML. Influence of tooth orientation on the detection of vertical root fracture in cone-beam computed tomography. J Endod 2018; 44: 1168-72.
23. Vanderstuyft T, Tarce M, Sanaan B, Jacobs R, de Faria Vasconcelos K, Quirynen M. Inaccuracy of buccal bone thickness estimation on cone-beam CT due to implant blooming: an ex-vivo study. J Clin Periodontol 2019; 46: 1134-43.
24. Wanderley VA, Nascimento EH, Gaêta-Araujo H, Oliveira-Santos C, Freitas DQ, Oliveira ML. Combined use of 2 cone-beam computed tomography scans in the assessment of vertical root fracture in teeth with intracanal material. J Endod 2021; 47: 1132-7.
25. Nascimento EH, Gaêta-Araujo H, Fontenele RC, Oliveira-Santos N, Oliveira-Santos C, Freitas DQ. Do the number of basis images and metal artifact reduction affect the production of artifacts near and far from zirconium dental implants in

CBCT? Clin Oral Investig 2021; 25: 5281-91.
26. Freitas DQ, Fontenele RC, Nascimento EH, Vasconcelos TV, Noujeim M. Influence of acquisition parameters on the magnitude of cone beam computed tomography artifacts. Dentomaxillofac Radiol 2018; 47: 20180151.
27. Queiroz PM, Oliveira ML, Groppo FC, Haiter-Neto F, Freitas DQ. Evaluation of metal artefact reduction in cone-beam computed tomography images of different dental materials. Clin Oral Investig 2018; 22: 419-23.